Impedance Control of a Teleoperated Mini Excavator

S.E. Salcudean, S. Tafazoli, P.D. Lawrence, and I. Chau
Department of Electrical & Computer Engineering
University of British Columbia
Vancouver, B.C. V6T 1Z4, Canada
tims@ee.ubc.ca

Abstract- A position-based impedance controller for excavator-type manipulators has been developed in our laboratory. This paper describes the proposed impedance controller and presents supporting experimental results. First, the problem of impedance control for a single hydraulic actuator is addressed and a method is presented for stability analysis. Steady-state position and force tracking of the closed loop system is also studied. Then, the desired impedance of the end-effector (bucket of the excavator) is mapped onto the hydraulic cylinders using the arm Jacobian and accurate estimates of the arm inertial and gravity terms. A non-conservative method is presented for predicting stability of the multivariable closed loop system. Experiments with an instrumented mini excavator (for the single cylinder case) show that the designed impedance controller has a good performance.

Keywords: impedance control, hydraulic excavator, contact experiments.

1. INTRODUCTION

The mini excavator is a heavy-duty human-operated hydraulic machine with a manipulator-like structure as shown in Figure 1. It is used for versatile construction operations such as digging, carrying loads, dumping loads, straight traction, and ground leveling. Traditionally, a human operator controls the main four links of the manipulator in joint-space coordinates through movements of two 2–DOF mechanical hand levers. Previous studies show that computer-assisted control results in improved performance and faster task completion for these types of machines [1–3]. In such an approach, the two hand levers are replaced by a 4–DOF joystick (three translational and one rotational degree of freedom). The operator is able to directly control the motion of the implement in Cartesian-space rather than coordinating the movements of all links to provide the desired endpoint (bucket) motion.

Most of the time, the excavator arm is required to carry out tasks involving contact with its environment such as digging and levelling. Although such tasks are commonly accomplished by operators using pure position control, the completion time and task quality is bound to improve with the use of computer-assisted compliance control. Active compliance can be provided by using either hybrid position/force control or impedance control [4]. In hybrid position/force control, the task space is divided into two orthogonal position and force controlled subspaces, while the objective of an impedance controller is to establish a desired dynamic relationship between the endpoint position and the environmental contact force, as introduced in [5]. To obtain impedance control, feedback loops at the manipulator joints are closed such that the robot appears as a specified impedance (target impedance) from the perspective of the environment.

A variety of control strategies have been developed in the literature for implementation of impedance control. Two common practical approaches are position-based and force-based impedance control [6]. The position-based impedance controller consists of an inner position-feedback loop and an outer force-feedback loop. The contact force information is used to modify the desired position of the end-effector that is applied to the inner position control loop. Thus, position-based impedance control can be viewed as a mechanism that softens a stiff position source using the contact force information. In contrast, the force-based impedance controller consists of an inner force-feedback loop and an outer position-feedback loop. Information from position sensors are used to modify the desired force trajectory that is applied to the inner loop. Thus, force-based impedance control can be viewed as a mechanism that stiffens a soft force source. The stability properties of these approaches has

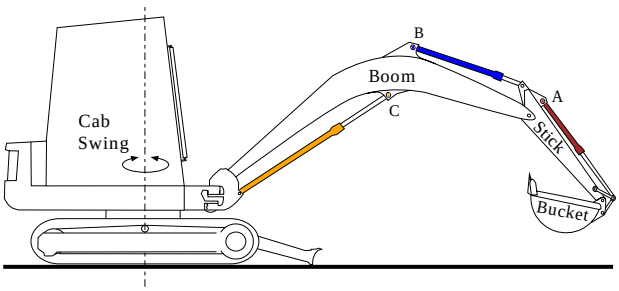

Figure 1. Schematic of the Takeuchi mini excavator.

been studied by Lawrence in [6].

To our best knowledge, the work reported by Heinrichs et al. in [7] is the only published work on impedance control of hydraulic actuators. The authors used a position-based impedance control scheme and presented a method for improving the inner position-control loop. In the present paper, we also propose the use of a position-based inner loop for the impedance control of a mini excavator. The contributions of this work can be summarized as follows:

(1) This is the first reported work on applying impedance control to an excavator arm.
(2) A novel approach is presented for predicting attainable range of impedances to preserve stability.
(3) A new method is presented for indirect measurement of the end-effector forces using load pin transducers.
(4) Performance of the proposed impedance controller is experimentally investigated on an instrumented mini excavator.

This paper is organized as follows: Instrumentation of the mini excavator is briefly explained in Section 2. Design and stability analysis of the single cylinder impedance controller is discussed in Section 3. Multi-link impedance control and corresponding stability analysis is addressed in Section 4. Experimental results on single cylinder impedance control are presented in Section 5. Conclusions and future work are outlined in Section 6.

2. THE INSTRUMENTED MINI EXCAVATOR

To perform closed loop control, several displacement, fluid pressure, and force sensors are required and the pilot stage of the main valves has to be modified. In this work, we only consider the three backhoe links[1]. The following sensors have been installed on each of the backhoe actuators :

- A digital resolver to measure the joint angle.
- A Temposonic® linear displacement sensor installed on the cylinder to measure cylinder extension.
- A load pin to measure the reaction force of the cylinder to its hinge. This sensor is sensitive to both tension and compression and is fixed to the link. In Figure 1, the load pins for the bucket, stick and boom are designated as A, B, and C, respectively.
- Two hydraulic pressure sensors to measure the line pressures.

[1] The term "backhoe" denotes the bucket, stick, and boom links shown in Figure 1.

The pilot stage of the main valves has been also modified to be able to control the machine by computer. A pair of fast on/off solenoid valves are installed in the pilot stage of each actuator. System identification experiments reported in our previous work verify that DPWM (Differential Pulse Width Modulation) operation of these valves at a 100 *Hz* frequency results in a reliable linear pilot system [8].

The sensors and the pilot valves are connected to a VMEbus based computer system, which consists of data-acquisition boards and a Sun SPARC 1E CPU board running VxWorks® real-time operating system. The computer system is networked to the local Ethernet and programs (written in C) are cross-developed in the UNIX environment.

In [9], we presented a method for indirect measurement of the joint torques of the mini excavator using load pin sensors. We also discussed that using load pins (instead of pressure transducers) for measuring actuator force, eliminates the error caused by the significant friction that exists inside the actuator seals. Least squares estimation of the link gravity terms (mass-related parameters) and analysis of the actuator friction were also reported in [9]. A comprehensive investigation of these issues can be found in [10].

3. SINGLE CYLINDER IMPEDANCE CONTROL

Figure 2 shows a hydraulic cylinder interacting with a mass-damper-spring environment. In this figure:

l = cylinder extension
f = force applied by the actuator to the load
l_e = displacement of the environment
f_e = force applied by the environment to the load
M_R = load mass
M_e, K_e, B_e = environmental parameters

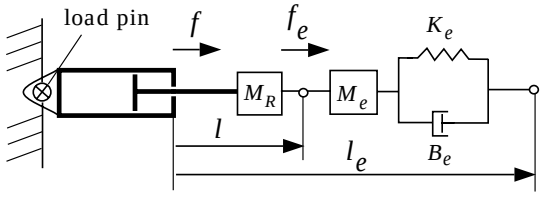

Figure 2. Hydraulic cylinder, load, and environment

According to Figure 1, both the stick and bucket actuators can be modeled as above. However, the boom load pin is connected to the end of its piston. The stick and bucket load pins measure the actuator force f, while the boom load pin directly measures the environmental force f_e. Impedance control of the boom cylinder can be studied in a manner similar to the analysis conducted in this section.

3.1. Cylinder Control as a Position Source

There are various nonlinearities that affect the dynamics of hydraulic actuators [11]. A number of approaches have been presented in the literature to compensate for these effects in position control design. For example, in [12], Vossoughi and Donath used the feedback linearization technique for this purpose. However, according to the experiments reported in Section 5, for our application, a simple PD controller results in an almost linear closed loop system with good position tracking performance. External forces (viewed as disturbances) have negligible effect on the position of the controlled actuator. Consequently, the closed loop system can be modeled as a position source described by the following linear equation:

$$l(s) = P(s)l_d(s), \qquad P(0) = 1 \tag{1}$$

where l_d is the desired cylinder extension. In Section 5, the transfer function P will be identified for the stick actuator from experimental data.

3.2. Position-Based Impedance Control

Suppose now that the actuator moves the load M_R against the environment shown in Figure 2. The environmental impedance can be described by the following equation:

$$-f_e = M_e s^2 l + (B_e s + K_e)(l - l_e) \tag{2}$$

Assume that the target impedance is given as follows:

$$f_e - f_{e0} = \big(M_D s^2 + B_D s + K_D\big)(l - l_0) \tag{3}$$

where, f_e is the actual environmental force and f_{e0} is the nominal (desired) environmental force on the cylinder load, and l_0 is the nominal (desired) cylinder extension. Modeling of the environmental and target impedance has been discussed in [13]. Newton's second law applied to the load, gives:

$$f + f_e = M_R s^2 l \tag{4}$$

By combining equations (3) and (4), one obtains the following position-force relationship for the cylinder:

$$\begin{aligned} &\big[(M_D - M_R)s^2 + B_D s + K_D\big]l = \\ &\big(M_D s^2 + B_D s + K_D\big)l_0 - f - f_{e0} \end{aligned} \tag{5}$$

Assuming that the cylinder behaves as a position/velocity source, and that the actuator force f is measured by the load pin, the relationship (5) can be implemented by setting the desired cylinder extension as follows:

$$\begin{aligned} l_d = \widehat{P^{-1}}(s)\,[\ &\frac{M_D s^2 + B_D s + K_D}{(M_D - M_R)s^2 + B_D s + K_D} l_0 \\ &- \frac{1}{(M_D - M_R)s^2 + B_D s + K_D}(f + f_{e0})\,] \end{aligned} \tag{6}$$

where $\widehat{P^{-1}}$ is a stable approximation to the inverse of P.

3.3. Stability Analysis

For the closed loop system, with $Q = P\widehat{P^{-1}}$, we have:

$$\begin{aligned} l = Pl_d = Q\,[\ &\frac{M_D s^2 + B_D s + K_D}{(M_D - M_R)s^2 + B_D s + K_D} l_0 \\ &- \frac{1}{(M_D - M_R)s^2 + B_D s + K_D}(f + f_{e0})\,] \end{aligned} \tag{7}$$

By combining equations (2) and (4), the following expression is obtained for the actuator force:

$$f = (M_e + M_R)s^2 l + (B_e s + K_e)(l - l_e) \tag{8}$$

The closed loop dynamics can be derived by replacing f in equation (7) with the above expression, which gives:

$$\begin{aligned} &\left[1 + Q\frac{(M_e + M_R)s^2 + B_e s + K_e}{(M_D - M_R)s^2 + B_D s + K_D}\right] l = \\ &Q\,[\ \frac{M_D s^2 + B_D s + K_D}{(M_D - M_R)s^2 + B_D s + K_D} l_0 \\ &+ \frac{B_e s + K_e}{(M_D - M_R)s^2 + B_D s + K_D} l_e \\ &- \frac{1}{(M_D - M_R)s^2 + B_D s + K_D} f_{e0}\ ] \end{aligned} \tag{9}$$

The Nyquist criterion can now be used to check the stability of the closed loop system. For $M_D \geq M_R$, since Q is stable, the overall system is stable as long as the polar plot of

$$Q\,\frac{(M_e + M_R)s^2 + B_e s + K_e}{(M_D - M_R)s^2 + B_D s + K_D} \tag{10}$$

does not encircle the $s = -1 + j0$ point.

Note that if P had a stable inverse, then $Q = 1$ and the characteristic equation of the closed loop system would be:

$$(M_e + M_D)s^2 + (B_e + B_D)s + (K_e + K_D) = 0 \tag{11}$$

3.4. Steady-State Tracking Accuracy

According to equation (9), in steady-state condition (at dc) we have:

$$l(0) = \frac{1}{1 + K_e/K_D}\left[l_0(0) + \frac{K_e}{K_D} l_e(0) - \frac{1}{K_D} f_{e0}(0)\right] \tag{12}$$

Therefore, as one can expect, position tracking is good if $K_D >> K_e$. The environmental force in the steady-state condition can be obtained from equation (2):

$$f_e(0) = K_e[l_e(0) - l(0)] \tag{13}$$

By combining equations (12) and (13), we obtain:

$$f_e(0) = \frac{1}{1 + K_D/K_e}[f_{e0}(0) + K_D(l_e(0) - l_0(0))] \tag{14}$$

Thus, as expected, the environmental force $f_e(0)$ tracks its desired value $f_{e0}(0)$ as long as $K_e >> K_D$. Force tracking in impedance control has been studied in [13].

4. TASK-SPACE IMPEDANCE CONTROL

The desired relationship between the bucket location and the force applied on it by environment can be described in most cases by the following matrix mass-damper-spring impedance:

$$f_{xe} - f_{xe0} = \big(M_D s^2 + B_D s + K_D\big)(x - x_0) \qquad (15)$$

where,

x = bucket position relative to the excavator base
x_0 = nominal (desired) bucket position
f_{xe} = environmental force applied to the bucket
f_{xe0} = nominal (desired) environmental force

The vectors of cylinder extensions l, arm joint angles q, load pin forces f, and joint torques τ are related by the following equations:

$$\begin{aligned} \dot{x} = J_R \dot{q} \quad &\rightarrow \quad \tau_e = J_R^T f_{xe} \\ \dot{q} = J_c \dot{l} \quad &\rightarrow \quad f = J_c^T \tau \\ D(q)\ddot{q} + C(q,\dot{q})\dot{q} + g(q) &= \tau + J_R^T f_{xe} \end{aligned} \qquad (16)$$

where, J_R is the excavator arm Jacobian, J_c is the Jacobian transformation (a diagonal matrix) relating cylinder extensions to joint angles, and the last equation describes the rigid-body dynamics of the excavator arm. For small velocities, the arm dynamics can be linearized at a given configuration as follows:

$$D(q)\ddot{q} + g(q) = \tau + J_R^T f_{xe} \qquad (17)$$

To transform from joint-space to cylinder-space, pre-multiply the above equation by J_c^T to obtain:

$$J_c^T D(q(l))\Big(J_c \ddot{l} + \dot{J}_c \dot{l}\Big) + J_c^T g(q(l)) = f + J_c^T J_R^T f_{xe} \qquad (18)$$

the term $\dot{J}_c \dot{l}$ is negligible at small velocities, therefore, the linearized dynamics in cylinder-space can be expressed as follows:

$$M_R \ddot{l} + J_c^T g - J^T f_{xe} = f \qquad (19)$$

where, $M_R \triangleq J_c^T D(q) J_c$ and $J \triangleq J_R J_c$.

4.1. Position-Based Impedance Control

Treating the Laplace variable s as differentiation operator, the Cartesian relationship specified by equation (15) can be transformed into cylinder-space as follows:

$$J^T(f_{xe} - f_{xe0}) = J^T\left(M_D s + B_D + K_D \frac{1}{s}\right) Js(l - l_0) \qquad (20)$$

Replacing for $J^T f_{xe}$ from equation (19), to obtain:

$$\begin{aligned} M_R s^2 l + J_c^T g - f - J^T f_{xe0} = \\ \big(J^T M_D J s^2 + J^T B_D J s + J^T K_D J\big)(l - l_0) \end{aligned} \qquad (21)$$

Thus, the desired impedance can be expressed by the following relationship in cylinder-space:

$$A_1(s) l = A_2(s) l_0 + J_c^T g - f - f_{e0} \qquad (22)$$

where $f_{e0} \triangleq J^T f_{xe0}$, and

$$A_1(s) \triangleq \big(J^T M_D J - M_R\big)s^2 + J^T B_D J s + J^T K_D J \qquad (23)$$

$$A_2(s) \triangleq J^T M_D J s^2 + J^T B_D J s + J^T K_D J \qquad (24)$$

As in the single cylinder case, assuming that the cylinders behave as velocity/position sources, the relationship (22) can be implemented by setting the desired cylinder extension vector to

$$l_d(s) = \widehat{P^{-1}}(s) A_1^{-1}(s)[A_2(s) l_0 + J_c^T g - f - f_{e0}]. \qquad (25)$$

where $\widehat{P^{-1}}$ is a stable approximation to the inverse of P, a diagonal matrix of cylinder transfer functions. As before, $Q = P\widehat{P^{-1}}$.

4.2. Stability Analysis

We assume the environmental dynamics to be described in the task-space by positive-definite matrix mass-damper-spring terms:

$$-f_{xe} = M_e s^2 x + (B_e s + K_e)(x - x_e) \qquad (26)$$

The cylinder-space linearized equations of motion are:

$$l = Q A_1^{-1}\big[A_2 l_0 + J_c^T g - f - f_{e0}\big] \qquad (27)$$

Replacing for f from equation (19) yields:

$$l = Q A_1^{-1}\big[A_2 l_0 + J^T f_{xe} - M_R s^2 l - f_{e0}\big] \qquad (28)$$

Using equation (26), the environmental force f_{xe} can be expressed in terms of the bucket position, which gives:

$$\begin{aligned} l = Q A_1^{-1}[A_2 l_0 - J^T M_e J s^2 l - \\ J^T (B_e s + K_e) J (l - l_e) - M_R s^2 l - f_{e0}] \end{aligned} \qquad (29)$$

The following closed loop dynamics is obtained by further manipulation:

$$\big[I + Q A_1^{-1} A_3\big] l = Q A_1^{-1}[A_2 l_0 + A_4 l_e - f_{e0}] \qquad (30)$$

where,

$$A_3(s) \triangleq \big(J^T M_e J + M_R\big)s^2 + J^T B_e J s + J^T K_e J \qquad (31)$$

$$A_4(s) \triangleq J^T B_e J s + J^T K_e J \qquad (32)$$

The multivariable Nyquist criterion (see [14]) can now be used to determine system stability.

5. EXPERIMENTAL RESULTS

This section reports the single cylinder experiments that were carried out using the stick actuator of the mini excavator. For this purpose, the stick piston was disconnected from the rest of the machine (to eliminate the structural dynamic effects) and was used in a horizontal orientation (to eliminate the gravity force). The Euler approximation was used for digital implementation of the controller at a sampling frequency of $f_s = 300Hz$. Experiments showed that sampling at a higher frequency does not improve the performance of the system any further.

5.1. Identification of the Position Control System

The employed position control law is as below:

$$u = K_p \Delta l + K_v \Delta \dot{l} + u_s \tag{33}$$

where $-5V \leqslant u \leqslant 5V$ is the applied voltage to the pilot stage of the stick actuator, $\Delta l = l_d - l$ is the positional tracking error, $\Delta \dot{l} = \frac{d}{dt}\Delta l$ is the velocity tracking error, $K_p = 100\,\frac{volt}{m}$ is the tuned position error gain, $K_v = 15\,\frac{volt}{m/s}$ is the tuned velocity error gain, and u_s is the additional term included to compensate for the deadband behavior of the main valve. It is experimentally set as follows:

$$u_s(\Delta l) = \begin{cases} +1.0V & \Delta l \geq 0 \\ -1.3V & \Delta l < 0 \end{cases} \tag{34}$$

Figure 3 shows the result of applying a low-pass-filtered white noise signal as the desired trajectory to the position control system. Note that this experiment corresponds to position control only.

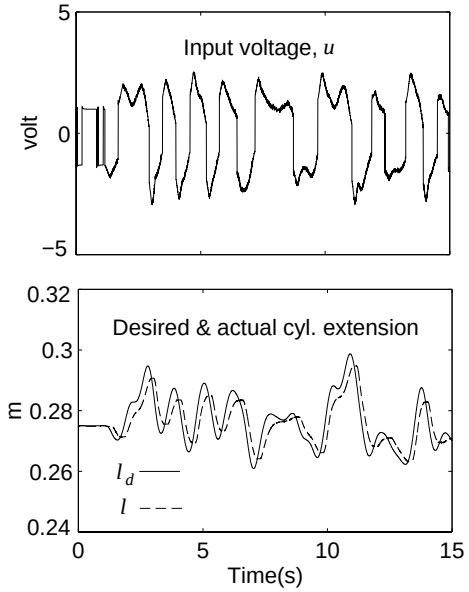

Figure 3. Position tracking performance.

Using least squares estimation (to estimate the parameter a), the following transfer function was obtained for the closed loop system:

$$P(s) = \frac{l(s)}{l_d(s)} = \frac{a}{s+a} = \frac{4.55}{s+4.55} \tag{35}$$

According to figure 4, the model predicts the system output with a good accuracy. Note that the inverse transfer function which is needed to implement the impedance controller, is the following PD term:

$$P^{-1}(s) = 1 + 0.22s \tag{36}$$

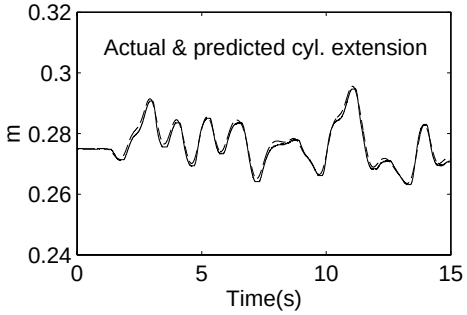

Figure 4. Model validation test.

5.2. Identification of the Environment

A strong rope was used to constrain the motion of the piston. In a position-controlled mode, the piston was commanded to enter the contact regime and respond to a low-pass-filtered white noise position input. Figure 5 shows the recorded load pin force and cylinder extension.

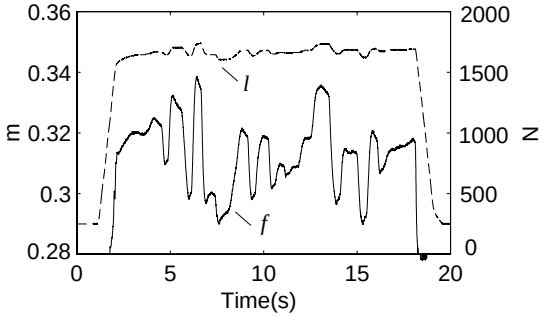

Figure 5. Environment identification test.

Least squares estimation was then used to estimate the damping and stiffness parameters of the environment from the experimental data. Note that the inertial effect of the environment is negligible:

$$K_e = 2.5 \times 10^5\ N/m, \quad B_e = 300\ Ns/m \tag{37}$$

Various experiments showed that the environment has nonlinear nature and the result of estimation depends on how much the rope is stretched. However, the above parameters can be used for approximate linear modeling of the rope environment.

5.3. Selection of the Impedance Parameters

Experiments showed that the inertial force measured by the load pin is quite negligible and we can assume that $M_R = 0$. Consequently, with $f_{e0} = 0$, the impedance control law of equation (6) can be simplified to:

$$l_d = P^{-1}(s)[l_0 - H(s)f] \tag{38}$$

where, $H(s)$ is the impedance filter defined as follows:

$$H(s) = \frac{1}{M_D\, s^2 + B_D\, s + K_D}. \tag{39}$$

The impedance parameters $M_D, B_D,$ and K_D can be chosen such that:

- The closed loop system has a desirable dynamics in the contact regime. This can be determined from the closed loop characteristic equation (11). Thus, an approximate estimate of the environmental parameters is required.
- The impedance filter is suitable. For example, the stiffness K_D is decided according to the desired compliance. Also, the filter response must be fast enough, so that in departure from contact regime, the desired position resumes its nominal value quickly.

Thus, for our application:

(1) The target stiffness was set to $K_D = 10^5\ N/m$.

(2) The target damping and inertia (M_D, B_D) were chosen such that the closed loop characteristic equation corresponds to a damping ratio of $\xi = 0.7$ and a natural frequency of $\omega_n = 30\, rad/s$. With this choice, the settling time would be $5/(\xi\omega_n) = 0.24s$. We have:

$$\begin{gathered}(K_D + K_e)/M_D = \left(10^5 + 2.5 \times 10^5\right)/M_D = \omega_n^2 = 900 \\ (B_D + B_e)/M_D = (B_D + 300)/M_D = 2\xi\omega_n = 42\end{gathered} \tag{40}$$

Thus, $M_D = 388.9\, Kg$ and $B_D = 1.61 \times 10^4\ Ns/m$.

(3) With the chosen parameters, the transfer function of the impedance filter becomes:

$$H(s) = \frac{0.0026}{(s + 33.79)\,(s + 7.61)} \tag{41}$$

This corresponds to an approximate settling time of $5/7.61 = 0.66\, s$, which is fast enough for our application.

5.4. Impedance Control Experiments

Figure 6 shows the result of applying a sinusoidal position trajectory where almost half of the trajectory falls into the contact regime. According to this figure, the impedance controller modifies the nominal trajectory in a proper manner and the closed loop system is stable. Figure 7 shows the result of an investigation to check whether the cylinder follows the target impedance or not. It is observed that matching between the position modification $(l_0 - l)$ and the filtered force $(H(s)f)$ is good.

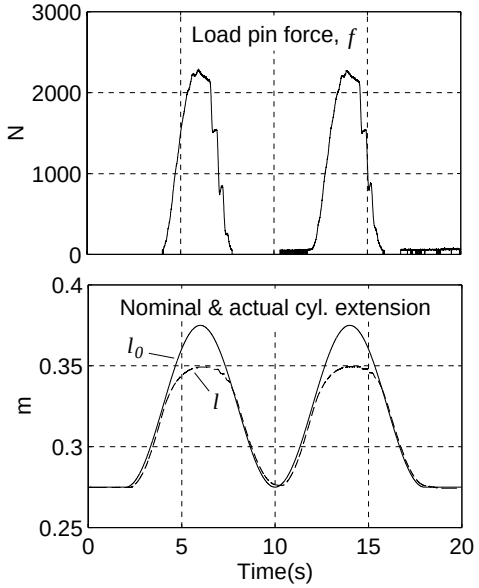

Figure 6. Impedance control experiment with a sinusoidal trajectory.

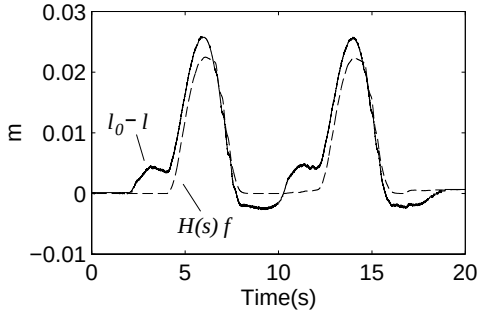

Figure 7. Impedance control validation test.

Figure 8 shows the result of applying a pulsed position trajectory to the system. This test is primarily intended to study the steady-state position tracking accuracy of the impedance controller. The jumps in steady-state conditions are:

$$\begin{gathered}\delta l_0 = 0.02\, m,\ \delta l = 0.0074\, m \\ \delta f = 1146.1\, N\end{gathered} \tag{42}$$

Thus, $K_e = \delta f/\delta l = 1.55 \times 10^5\, N/m$, which is considerably lower than what was obtained from least squares estimation. The main reason is believed to be the nonlinear behavior of the environment. From equation (12), the relative jump in position has to be $1/(1 + K_e/K_D) = 0.392$ and from the recorded signals we read $\delta l/\delta l_0 = 0.370$.

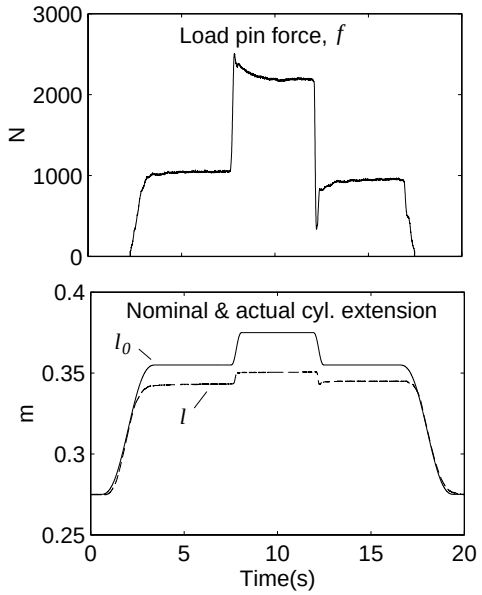

Figure 8. Experiment with a pulsed trajectory.

6. CONCLUSION

A novel approach was presented in this paper for position-based impedance control of excavator arms. In this approach, the position-controlled hydraulic cylinder was modeled as a position source and the measured contact force (using load pin) was used to modify the desired trajectory. We showed that closed loop stability can be checked using Nyquist criterion. Single cylinder experiments were carried out to identify the position control system, to estimate the environmental parameters, and also to investigate the performance of the impedance controller. The experimental results validated the theoretical findings and showed that the designed impedance controller is a suitable one. Task-space experimental results will appear in our future work.

Acknowledgments- The financial support for this work was provided by IRIS-II Project IS-4. We wish to thank Keyvan Hashtrudi-Zaad for his careful reading of the manuscript and Simon Bachmann for his help with the machine hardware.

REFERENCES

[1] N. Sepehri, P.D. Lawrence, F. Sassani and R. Frenette, "Resolved-mode teleoperated control of heavy-duty hydraulic machines," *Journ. Dyn. Sys., Meas. and Contr., Trans. ASME,* vol. 116, pp. 232–240, Jun 1994.

[2] P.D. Lawrence, S.E. Salcudean, N. Sepehri, D. Chan, S. Bachmann, N. Parker, M. Zhu and R. Frenette, "Coordinated and force-feedback control of hydraulic excavators," *in Proc. 4th Int. Symp. on Exp. Robotics, ISER' 95,* Stanford, CA, pp. 114–121, Jun 1995.

[3] N.R. Parker, S.E. Salcudean and P.D. Lawrence, "Application of force feedback to heavy duty hydraulic machines," *in Proc. IEEE Int. Conf. on Robotics and Automation,* pp. 375–381, 1993.

[4] M. Vukobratovic and A. Tuneski, "Contact control concepts in manipulation robotics - an overview," *IEEE Trans. on Industrial Electronics,* vol. 41, no. 1, pp. 12–24, Feb 1994.

[5] N. Hogan, "Impedance control: an approach to manipulation, parts I-III," *Journ. Dyn. Sys., Meas., and Contr., Trans. ASME,* vol. 107, pp. 1–24, Mar 1985.

[6] D.A. Lawrence, "Impedance control stability properties in common implementations," *in Proc. IEEE Int. Conf. on Robotics and Automation,* pp. 1185–1190, 1988.

[7] B. Heinrichs, N. Sepehri and A.B. Thornton-Trump, "Position-based impedance control of an industrial hydraulic manipulator," *IEEE Contr. Sys. Mag.,* vol. 17, no. 1, pp. 46–52, Feb 1997.

[8] S. Tafazoli, P. Peussa, P.D. Lawrence, S.E. Salcudean and C.W. de Silva, "Differential PWM operated solenoid valves in the pilot stage of mini excavators: modeling and identification," *in Proc. ASME Int. Mech. Eng. Congr. and Expos., FPST-3,* Atlanta, GA, pp. 93–99, Nov 1996.

[9] S. Tafazoli, P.D. Lawrence, S.E. Salcudean, D. Chan, S. Bachmann and C.W. de Silva, "Parameter estimation and friction analysis for a mini excavator," *in Proc. IEEE Int. Conf. on Robotics and Automation,* Minneapolis, Minnesota, vol. 1, pp. 329–334, Apr 1996.

[10] S. Tafazoli, "Identification of frictional effects and structural dynamics for improved control of hydraulic manipulators," Ph.D. Thesis, Elect. & Comp. Eng. Dept., University of British Columbia, Jan 1997.

[11] H.E. Merritt, *Hydraulic Control Systems.* New York, NY: John Wiley & Sons Inc., 1967.

[12] G. Vossoughi and M. Donath, "Dynamic feedback linearization for electrohydraulically actuated control systems," *Journ. Dyn. Sys., Meas., and Contr., Trans. ASME,* vol. 117, pp. 468–477, Dec 1995.

[13] H. Seraji and R. Colbaugh, "Force tracking in impedance control," *The Int. Journ. of Robotics Research,* vol. 16, no. 1, pp. 97–117, Feb 1997.

[14] J.M. Maciejowski, *Multivariable Feedback Design.* Addison-Wesley, 1989.